Published in final edited form as:
Nat Immunol. 2012 September ; 13(9): 832–842. doi:10.1038/ni.2376.

Tumor-infiltrating DCs suppress nucleic acid–mediated innate immune responses through interactions between the receptor TIM-3 and the alarmin HMGB1

Shigeki Chiba[1], **Muhammad Baghdadi**[1,2,3], **Hisaya Akiba**[4], **Hironori Yoshiyama**[1], **Ichiro Kinoshita**[3], **Hirotoshi Dosaka-Akita**[3], **Yoichiro Fujioka**[5], **Yusuke Ohba**[5], **Jacob V Gorman**[6], **John D Colgan**[6], **Mitsuomi Hirashima**[7], **Toshimitsu Uede**[8], **Akinori Takaoka**[2], **Hideo Yagita**[4], and **Masahisa Jinushi**[1]

[1]Research Center for Infection-Associated Cancer, Institute for Genetic Medicine, Hokkaido University, Sapporo, Japan.

[2]Division of Signaling on Cancer and Immunology, Institute for Genetic Medicine, Hokkaido University, Sapporo, Japan.

[3]Department of Medical Oncology, Hokkaido University Graduate School of Medicine, Sapporo, Japan.

[4]Department of Immunology, Juntendo University School of Medicine, Tokyo, Japan.

[5]Department of Pathophysiology and Signal Transduction, Hokkaido University Graduate School of Medicine, Sapporo, Japan.

[6]Department of Internal Medicine, University of Iowa, Iowa City, Iowa, USA.

[7]Department of Immunology and Immunopathology, Faculty of Medicine, Kagawa University, Kagawa, Japan.

[8]Division of Molecular Immunology, Institute for Genetic Medicine, Hokkaido University, Sapporo, Japan.

Abstract

The mechanisms by which tumor microenvironments modulate nucleic acid–mediated innate immunity remain unknown. Here we identify the receptor TIM-3 as key in circumventing the stimulatory effects of nucleic acids in tumor immunity. Tumor-associated dendritic cells (DCs) in mouse tumors and patients with cancer had high expression of TIM-3. DC-derived TIM-3 suppressed innate immune responses through the recognition of nucleic acids by Toll-like receptors and cytosolic sensors via a galectin-9-independent mechanism. In contrast, TIM-3 interacted with the alarmin HMGB1 to interfere with the recruitment of nucleic acids into DC endosomes and attenuated the therapeutic efficacy of DNA vaccination and chemotherapy by

Correspondence should be addressed to M.J. (jinushi@igm.hokudai.ac.jp)..

AUTHOR CONTRIBUTIONS

M.J. and H.Ya. designed the experiments; S.C., M.B., H.A., H.Yo., Y.F. and M.J. prepared reagents and did the experiments; S.C., M.B., H.A., H.Yo., Y.F., Y.O., J.D.C., M.H., T.U., A.T., H.Ya. and M.J. analyzed and discussed the data; I.K. and H.D.-A. provided clinical samples; H.A., J.V.G., J.D.C., M.H. and H.Ya. developed new materials; and M.J. was responsible for the overall study design and writing the manuscript.

Note: Supplementary information is available in the online version of the paper.

COMPETING FINANCIAL INTERESTS

The authors declare no competing financial interests.

diminishing the immunogenicity of nucleic acids released from dying tumor cells. Our findings define a mechanism whereby tumor microenvironments suppress antitumor immunity mediated by nucleic acids.

Accumulating evidence has demonstrated the potential of endogenous immune responses in modulating the clinical outcome of malignant diseases[1,2]. Thus, manipulation of the immune system should enable enhancement of the therapeutic effects of the present anticancer modalities[3,4]. However, oncogenic and epigenetic alterations of tumor cells often adopt multiple strategies to form complex networks with tumor-infiltrating cells, which leads to the impairment of efficient tumor immunosurveillance[5,6].

Innate immunity serves as a first line of defense against infectious agents, and germline-encoded pattern-recognition receptors (PRRs) detect stressed and infected cells and elicit potent effector activities that achieve efficient containment of microbes[7]. Among the specialized subsets of cells of the innate immune system, dendritic cells (DCs) are particularly important as critical sensors through their wide expression of various PRRs[8]. These pattern-sensing systems on DCs are also applicable to the recognition of tumor-derived stress-related factors. In particular, Toll-like receptors (TLRs) and cytosolic sensors for DNA and RNA recognition expressed by DCs use endogenous host elements carrying microbial components (such as the alarmin HMGB1), pathogen-associated molecular patterns and/or nucleic acids to stimulate intrinsic apoptotic pathways to generate protective immune responses to nascent tumors[9–11]. However, how DCs regulate PRR-mediated innate immune systems in tumor microenvironments and thus how they affect anticancer therapies remain largely unknown.

Here we identify the receptor TIM-3 on DCs as a key factor in circumventing nucleic acid–mediated activation of the innate immune system. TIM-3 was initially identified as a negative regulator of T helper type 1 immunity after ligation of galectin-9 (refs. 12–14). However, TIM-3 is also expressed on myeloid cells such as monocytes and macrophages[15,16], but whether TIM-3 on DCs has a role in the regulation of antitumor immunity has remained largely unknown. We found here that DCs in tumor microenvironments had higher expression of TIM-3 than did DCs in normal tissues. Furthermore, TIM-3 on tumor-associated DCs (TADCs) suppressed PRR-mediated innate immune responses to nucleic acids by interfering with HMGB1-mediated activation of nucleic acid–sensing systems. Our findings define a mechanism by which tumor microenvironments impede the immunological responses of DCs to nucleic acid adjuvants, which results in impaired antitumor immunosurveillance and therapy.

RESULTS

High expression of TIM-3 by tumor-infiltrating DCs

To explore a potential role for TIM-3 in regulating antitumor responses, we examined its expression on myeloid cells from mice bearing 3LL Lewis lung cancer tumors or MC38 colorectal adenocarcinoma tumors. Among single-cell suspensions prepared from subcutaneous tumors, $CD11c^{hi}$ conventional DCs, $CD11c^{lo}B220^{+}PDCA1^{+}$ plasmacytoid DCs and $CD11b^{+}F4/80^{+}$ tumor-associated macrophages had high TIM-3 expression, but $CD11b^{+}Gr\text{-}1^{+}$ myeloid-derived suppressor cells did not (**Fig. 1a** and **Supplementary Fig. 1a**). In contrast, few TIM-3-expressing DCs or macrophages were present in the tumor-draining or distal lymph nodes and spleens of tumor-bearing mice or in mice without tumors (**Fig. 1a**). In line with tumor-specific expression of TIM-3, we also detected TIM-3 on tumor cells *in situ* and tumor-infiltrating $CD8^{+}$ T cells but not on splenic $CD8^{+}$ T cells of tumor-bearing mice. In contrast, we did not detect TIM-3 on mouse tumor cell lines cultured *in*

vitro (**Supplementary Fig. 1b,c**), which indicated that tumor micro-environments may have a role in the regulation of TIM-3 expression on both the tumor and host leucocytes. However, TIM-3 was expressed on *in vitro*–cultured human non-small-cell lung carcinoma (NSCLC) tumor lines and primary $EpCAM^+$ NSCLC epithelial tumor cells from patients with cancer (**Supplementary Fig. 1d,e**). TIM-3 had much higher expression and was expressed at earlier times on TADCs than on tumor-infiltrating $CD8^+$ T cells after subcutaneous tumor challenge (**Fig. 1b**). In contrast, TIM-3 expression in $CD8^+$ T cells gradually increased and reached its maximum of about 50% of that in total $CD8^+$ T cells by 4 weeks after tumor challenge (**Fig. 1b**). These results suggested that the tumor microenvironment induced DCs to express TIM-3 with kinetics different from those of $CD8^+$ T cells.

To investigate possible tumor-derived factors that contributed to the high expression of TIM-3 by DCs, we incubated immature bone marrow–derived dendritic cells (BMDCs) overnight with mouse tumor cells or with tumor-cell supernatants. TIM-3 expression was much higher after coculture with tumor cells or treatment with culture supernatants than after culture in medium alone (**Fig. 1c,d**). Various factors derived mainly from tumor cells and their microenvironments bestow tumorigenic activities on DCs by inducing their expression of tumor-promoting and immunosuppressive factors, such as arginase I, indoleamine 2,3-deoxygenase, interleukin 10 (IL-10), transforming growth factor-β1 (TGF-β1) and vascular endothelial growth factor (VEGF)[17–19]. Although 3LL tumors treated individually with inhibitors of the VEGF receptor VEGF-R2, IL-10 or arginase I had marginal inhibitory effects on TIM-3 expression when added to BMDCs (**Supplementary Fig. 2a**), treatment with a combination of all three inhibitors largely diminished the upregulation of TIM-3 on BMDCs mediated by tumor-cell supernatants (**Fig. 1d**). Moreover, TIM-3 on BMDCs was upregulated substantially by recombinant IL-10 or VEGF-A alone or together, in a dose-dependent manner (**Supplementary Fig. 2b**).

In contrast to the results noted above, TIM-3 was not upregulated on mouse 3LL NSCLC tumor cells treated with VEGF-A and IL-10 (**Supplementary Fig. 2c**), which suggested that tumor cells use mechanisms to induce their expression of TIM-3 distinct from those used by DCs. Thus, TIM-3 expression on DCs was regulated by the synergistic actions of multiple immunoregulatory factors released from tumor cells. In addition, we also detected high expression of TIM-3 on the surface of $CD11c^+$ TADCs from patients with advanced NSCLC, gastric adenocarcinoma or neuroendocrine tumors but not on DCs differentiated from peripheral blood monocytes of patients or healthy volunteers (**Fig. 1e**). Thus, we detected high expression of TIM-3 specifically on DCs from both mouse and human tumor microenvironments.

TIM-3 suppresses innate responses to nucleic acids

We next evaluated the role of TIM-3 in DC function. For this, we isolated the $TIM\text{-}3^+$ population of bulk BMDCs, as TIM-3 is expressed on only a small portion (~5–10%) of BMDCs differentiated with granulocyte-monocyte colony-stimulating factor. $TIM\text{-}3^+$ DC populations included more mature $CD11c^{hi}CD86^{hi}$ cells than did their $TIM3^-$ counterparts. However, their ability to cross-prime ovalbumin-specific T cells was similar to that of the $TIM\text{-}3^-$ DCs (data not shown).

Given reports indicating that TIM-3 on antigen-presenting cells acts together with TLR signals to trigger inflammatory signals[15], we examined the role of TIM-3 in the regulation of TLR-mediated innate immune responses. Expression of the cytokines interferon-β1 (IFN-β1), IFN-α4, IL-6 and IL-12 was much lower in $TIM\text{-}3^+$ DCs isolated from wild-type BMDCs than in $TIM\text{-}3^-$ DCs isolated from TIM-3-deficient BMDCs after stimulation with

nucleic-acid agonists for TLR3 (the synthetic RNA duplex poly(I: C)), TLR7 (the synthetic imidazoquinoline resiquimod (R-848)) and TLR9 (the dinucleotide CpG-ODN) but not after stimulation with agonists for TLR2 (peptidoglycan) or TLR4 (lipopolysaccharide; **Fig. 2a** and **Supplementary Fig. 3a**). As TLR3, TLR7 and TLR9 serve as pattern-recognition sensors for double-stranded RNA, single-stranded RNA and single-stranded DNA, respectively, we hypothesized that TIM-3 might be broadly involved in the regulation of nucleic acid–mediated immune responses. Indeed, cytokine secretion by wild-type TIM-3^+ BMDCs was much lower than that by TIM-3-deficient TIM-3^- BMDCs after stimulation via transfection of synthetic B-form double-stranded DNA (poly(dA:dT); B-DNA) or interferon-stimulatory DNA, which are ligands for sensors of cytosolic DNA, as well as after stimulation with poly(I:C) or triphosphate RNA, which are ligands for the RNA sensors Mda5 and RIG-I (**Fig. 2a**). Moreover, treatment with monoclonal antibody (mAb) to TIM-3 or small interfering RNA targeting TIM-3 expression resulted in much more IFN-β protein in wild-type TIM-3^+ DCs in response to agonists for cytosolic sensors or TLRs (**Fig. 2b**). Blockade of TIM-3 also augmented IFN-β1 expression in TIM-3^+ DCs derived from wild-type mice, but not those from TIM-3-deficient mice, after treatment with plasmid encoding either of the melanoma-differentiation antigens TRP-2 or gp100 or plasmid with no insert (**Fig. 2c** and data not shown), which indicated that the tumor antigen–encoding sequence was dispensable for the DNA-induced innate immune responses.

To delineate the contribution of TIM-3 to nucleic acid–mediated innate immune responses, we transfected TIM-3^- mouse embryonic fibroblasts (MEFs) with control vector or vector expressing TIM-3. TIM-3 expression led to less cytokine production by MEFs in response to B-DNA, genomic DNA isolated from tumors (B16 mouse melanoma or EL-4 mouse lymphoma) or pathogens, including *Escherichia coli*, *Helicobacter pylori* and human cytomegalovirus (**Fig. 2d** and **Supplementary Fig. 3b**). We also observed TIM-3-mediated suppression of innate responses to bacterial and viral DNA in BMDCs (data not shown). Moreover, luciferase reporter assays of HEK293 human embryonic kidney cells showed that TIM-3 suppressed the B-DNA-induced activity of the transcription factors IRF3 and NF-κB, which serve as essential components of TLR- and cytosolic sensor–mediated responses (**Fig. 2e**).

To determine whether TIM-3 negatively regulated innate immune responses to nucleic acids *in vivo*, we measured IFN-β1 mRNA and IL-12 mRNA in TADCs isolated from tumor-bearing mice or patients with cancer. TADCs had a lower abundance of transcripts for IFN-β1 and IL-12 and less secretion IFN-β1 and IL-12 protein induced by control plasmid with no insert (empty vector; called ‘control plasmid DNA’ here) than did splenic DCs or DCs differentiated from peripheral blood monocytes, but treatment with mAb to TIM-3 resulted in higher cytokine expression and more release of cytokines to an even greater degree in TADCs than in splenic DCs or DCs differentiated from peripheral blood monocytes (**Fig. 2f,g**).

Consistent with a critical role for DC-derived TIM-3 in restraining immune responses to nucleic acids, TIM-3 strongly suppressed cytokine production by $CD11c^{lo}B220^+$ plasmacytoid DCs in a manner similar to that seen with $CD11c^{hi}$ conventional DCs infiltrating into tumor tissue. The upregulation of the expression of IFN-β and IL-12 mediated by mAb to TIM-3 was much greater in $CD11c^{hi}$ DCs or $CD11c^{lo}B220^+$ plasmacytoid DCs than in tumor-associated macrophages or myeloid-derived suppressor cells isolated from tumor tissue, whereas upregulation of the expression of TIM-3 was similar among these cells of the myeloid lineage (**Supplementary Figs. 1a** and **3c**). Blockade of TIM-3 had little effect on innate responses in TIM-3^{hi} tumor-infiltrating $CD8^+$ T cells after stimulation with CpG-ODN (data not shown). Together these results

demonstrated that TIM-3 resulted in much less activation of TADCs by interfering with their recognition of and response to normally immunostimulatory nucleic acids.

DC-specific TIM-3 perturbs the antitumor efficacy of DNA

To examine the effect of TIM-3 on nucleic acid–mediated antitumor responses, we used various nucleic acid–based adjuvants, including control plasmid DNA or plasmid encoding TRP-2 (ref. 20), as well as the TLR9 agonist CpG-ODN, as therapeutic options for established mouse tumors. Immunization with control plasmid DNA partially lowered the tumor burden caused by the more aggressive B16-F10 variant of the B16 melanoma. Although mAb to TIM-3 alone afforded a small delay in tumor growth, it eventually failed to protect mice from developing tumors (**Fig. 3a**). In contrast, combined treatment with control plasmid DNA and mAb to TIM-3 resulted in substantial inhibition of tumor growth (**Fig. 3a** and data not shown). These results suggested that TIM-3 exerted a marginal effect because the release of endogenous DNA in untreated tumors was limited, but exogenous DNA administered therapeutically triggered a strong antitumor effect after blockade of TIM-3. Blockade of TIM-3 delayed tumor growth to a similar extent in combination with either control plasmid with no insert or TRP-2-encoding plasmid (data not shown), which suggested that TIM-3 regulated innate immune responses independently of a particular tumor antigen. Consistent with that, blockade of TIM-3 induced the antitumor activity of the plasmid encoding TRP-2 but not of a vaccine consisting of TRP-2 peptide (**Fig. 3a** and data not shown). Tumors from mice treated with both plasmid DNA and mAb to TIM-3 had more IFN-β and IL-12 protein than did those from mice treated with mAb to TIM-3 or DNA alone (**Fig. 3b**), which indicated the close relationship between cytokine concentrations and antitumor effects.

To further define the role of DC-derived TIM-3 in circumventing the therapeutic efficacy of DNA vaccines, we treated B16-F10 melanomas with plasmid DNA and mAb to TIM-3 in CD11c-DTR mice, in which conditional depletion of $CD11c^+$ DCs can be achieved by administration of diphtheria toxin. In CD1c-DTR mice not treated with diphtheria toxin that had endogenous $TIM\text{-}3^{hi}$ TADCs, control plasmid DNA plus mAb to TIM-3 protected mice from growing tumors more than control plasmid DNA alone did (**Fig. 3c**). In contrast, depletion of DCs from CD11c-DTR mice resulted in much greater antitumor effects of DNA alone in this model (**Fig. 3c**). To elucidate whether TIM-3 on DCs impeded antitumor responses mediated by nucleic acids, we adoptively transferred wild-type or TIM-3-deficient BMDCs into DC-deficient CD11c-DTR mice with B16-F10 melanoma. Treatment with control plasmid DNA was ineffective against established B16-F10 tumors in the presence of wild-type DCs, whereas treatment with control plasmid DNA induced profound inhibition of tumor growth after transfer of TIM-3-deficient DCs (**Fig. 3d**).

To further define the role of TIM-3 expressed on endogenous DCs in the antitumor effect of DNA adjuvant, we generated mixed–bone marrow chimeras that could be selectively depleted of TIM-3-expressing DCs from CD11c-DTR mice. We mixed bone marrow cells from TIM-3-deficient mice and CD11c-DTR mice at a ratio of 1:1 and used that mixture to reconstitute irradiated wild-type recipient mice, then compared the antitumor effects of control plasmid DNA in those chimeras treated with diphtheria toxin or not. Treatment with DNA alone restrained tumor growth more potently in diphtheria toxin–treated chimeras than in those not treated with diphtheria toxin, whereas mAb to TIM-3 had an inhibitory effect on tumor growth regardless of treatment with diphtheria toxin (**Fig. 3e**). Together these findings further exemplified the role of DC-specific TIM-3 in negatively regulating nucleic acid–mediated antitumor immunity. We observed similar synergistic antitumor effects of DNA and mAb to TIM-3 in mice of the nonobese diabetic–severe combined immunodeficiency (NOD-SCID) strain and C57BL/6 mice treated with depleting antibody

to CD8 (anti-CD8) or control immunoglobulin (**Supplementary Fig. 4**). These results further confirmed that TIM-3 on $CD8^+$ T cells was not responsible for the synergistic activities of DNA and mAb to TIM-3, which differed from published observations suggesting that $CD8^+$ T cells are necessary for the exertion of antitumor responses induced by mAb to TIM-3 alone[21].

To determine the mechanisms by which the blockade of TIM-3 elicited antitumor responses, we focused on the contributions of type I interferon and IL-12 to the nucleic acid–triggered responses, because these are well-known antitumor effector cytokines. Indeed, the antitumor effect of control plasmid DNA was mostly abolished in diphtheria toxin–treated CD11c-DTR mice when the control plasmid DNA was administered together with neutralizing mAb to the receptor for type I interferon (IFN-IR) and mAb to IL-12. Moreover, the antitumor effect of mAb to TIM-3 and control plasmid DNA was also abrogated by the combined blockade of IFN-IR and IL-12 in CD11c-DTR mice not treated with diphtheria toxin or in NOD-SCID mice (**Fig. 4a–c**). Treatment with neutralizing antibody to IFN-IR, to IL-12 or to both had little effect on the growth of B16-F10 tumors in the absence of the administration of control plasmid DNA (data not shown), which indicated that immunogenic DNA was required for the triggering of antitumor responses by IFN-IR and IL-12.

$CD11c^{lo}B220^+PDCA1^+$ plasmacytoid DCs, $CD11c^{hi}$ conventional DCs, $F4/80^+CD11b^+$ macrophages and $CD45^-gp38^+$ stromal cells were the main producers of type I interferon and IL-12 in the tumor microenvironments of NOD-SCID mice after treatment with control plasmid DNA and mAb to TIM-3 (**Fig. 4d**). Moreover, cytotoxic activity was much greater in natural killer cells, macrophages and plasmacytoid DCs of NOD-SCID mice treated with control plasmid DNA and mAb to TIM-3 than in those of mice treated with control plasmid DNA alone (**Fig. 4e**), consistent with published reports that the appropriate innate immune adjuvants may trigger the antitumor effector functions of plasmacytoid DCs[22]. In CD11c-DTR mice depleted of DCs, the main sources of IFN-β1 and IL-12 were macrophages and $CD45^-$ stromal cells, and natural killer cells and macrophages were main effectors involved in killing tumor cells in an IFN-IR- and IL-12-dependent manner (data not shown). Together these results suggested that blockade of TIM-3 might convert tolerogenic cells of the innate immune system into antitumor effector cells and that type I interferon and IL-12, as well as various innate cells, act as downstream effectors to trigger antitumor responses mediated by DNA and mAb to TIM-3.

TIM-3 regulates innate response independently of galectin-9

The interaction between galectin-9 and TIM-3 on myeloid cells elicits antimicrobial and antitumor immunity but inhibits T helper type 1 responses[23–25]. However, treatment with recombinant galectin-9 or mAb to galectin-9 did not suppress B-DNA-mediated cytokine production in $TIM\text{-}3^+$ or $TIM\text{-}3^-$ DCs (**Fig. 5a,b**). We detected much less galectin-9 mRNA in TADCs and tumor cells than in splenic DCs derived from tumor-bearing or normal mice (**Fig. 5c**). Bulk tumor tissues also had significantly less galectin-9 mRNA than did normal tissues in B16 tumor–bearing mice (**Fig. 5d**), which indicated that galectin-9 production was compromised in tumors. Furthermore, treatment with mAb to galectin-9 did not enhance the antitumor effects of control plasmid DNA (**Fig. 5e**).

In addition to galectin-9, phosphatidylserine exposed by apoptotic cells is a TIM-3 ligand[26,27]. However, treatment with annexin V, which also binds phosphatidylserine and potentially competes with TIM-3, had little effect on B-DNA-mediated expression of the gene encoding IFN-β1 in $TIM\text{-}3^+$ MEFs (**Fig. 5f**), which suggested that TIM-3-mediated regulation of nucleic acid sensing was independent of the recognition of phosphatidylserine on apoptotic cells. Together these findings demonstrated that DC-derived TIM-3 recognized

a ligand other than galectin-9 or phosphatidylserine to suppress nucleic acid–mediated immune responses.

TIM-3 serves as a receptor for HMGB1

In HEK293 cells, B-DNA is recognized by the intracellular receptor RIG-I through the induction of an RNA polymerase III–transcribed RNA intermediate[28]. TIM-3 had little inhibitory effect on the IFN-β1 response in HEK293 cells transfected with expression vectors for RIG-I or the signaling adapters STING, MAVS, MyD88 and TRIF (data not shown). This indicated that TIM-3 acted on nucleic acid–sensing systems upstream of PRR-specific pathways.

HMGB1 is an evolutionarily conserved nuclear protein that acts on various cells and interacts with many different types of ligands, such as RAGE, TLR4 and so on, to modulate pleiotropic functions of these entities in various physiological and pathological situations[29]. HMGB1 also has an essential role in activating innate immune responses mediated by sensors of nucleic acids[30,31]; therefore, we investigated potential interactions between HMGB1 and TIM-3. We indeed found that TIM-3 bound HMGB1 with an affinity similar to that of RAGE, a known receptor for HMGB1 (**Fig. 6a**). Furthermore, the interaction between HMGB1 and TIM-3 was partially suppressed in the presence of a fusion of RAGE and the Fc portion of immunoglobulin or galectin-9 protein (**Supplementary Fig. 5a**), which confirmed the specificity of the interaction between HMGB1 and TIM-3 in this analysis.

TIM-3 binds phosphatidylserine through a metal ion–dependent ligand-binding site in its FG loop[32,33]. We therefore constructed a fusion of mutant TIM-3 and the Fc portion of immunoglobulin, with the glutamine at position 62 near the FG loop of TIM-3 (at the galectin-9-independent ligand-binding site) replaced with alanine (Tim-3(Q62A)–Fc)[32]. This substitution largely abrogated the ability of TIM-3 to bind HMGB1 (**Fig. 6a**), which indicated that the metal ion–dependent ligand-binding portion of TIM-3 was critical for binding HMGB1. In addition, the interaction of a fusion of wild-type TIM-3 and Fc (TIM-3(WT)–Fc) with HMGB1 was blocked by mAb to TIM-3 (**Fig. 6b**).

HMGB1 has DNA-binding domains in its A-box and B-box, and its interaction with DNA is enhanced by the tail domain at its carboxyl terminus[29]. Thus, we determined whether TIM-3 and nucleic acids competed for binding to the same domain of HMGB1. Indeed, the binding of either B-DNA or TIM-3 (WT)–Fc to HMGB1 was mostly abrogated by deletion of the A-box but not by deletion of the B-box or carboxy-terminal domain (**Supplementary Fig. 5b,c**). Furthermore, the binding of biotin-labeled B-DNA to HMGB1 was inhibited by unlabeled TIM-3 (WT)–Fc in a concentration-dependent manner. In contrast, unlabeled TIM-3(Q62A)–Fc did not inhibit the interaction between B-DNA and HMGB1 (**Fig. 6c**), which indicated that TIM-3 and nucleic acids competed with each other for binding to A-box domain of HMGB1.

Moreover, wild-type TIM-3^+ DCs interacted with biotin-labeled HMGB1 with a higher affinity than that of wild-type TIM-3^- DCs, although both were inhibited by mAb to TIM-3 (**Fig. 6d**). There was detectable binding of HMGB1 to TIM-3^- DCs, although it was much lower than the binding of HMGB1 to their TIM-3^+ counterparts (**Fig. 6d**), which suggested that some other receptors, such as RAGE, may have been involved in the binding of HMGB1 to TIM-3^- DCs. TIM-3 was also located together with HMGB1 in TIM-3^+ DCs (**Fig. 6e**) and bound to HMGB1 in MEFs transfected to express TIM-3. Furthermore, densitometry of immunoprecipitated bands showed that the inhibitory effect of mAb to TIM-3 on this binding was significant (**Fig. 6f**). Tumors had significantly more HMGB1 mRNA than did normal tissues (**Fig. 6g**), which indicated that in contrast to galectin-9

production, HMGB1 production occurred in tumors. Together these results identified TIM-3 as a putative receptor for HMGB1 in DCs in tumor microenvironments.

TIM-3 inhibits the recruitment of nucleic acids into endosomes

Proper trafficking of nucleic acids into endosomal vesicles is a key event in the initiation of innate immune signaling. Danger-associated molecules such as uric acid and HMGB proteins form complexes with nucleic acids and allow them access to endosomal vesicles and allow the triggering of immune responses[34]. We therefore investigated whether HMGB1 directly affected the recruitment of nucleic acids into endosomal vesicles. For this, we adopted an experimental system of HMGB1-deficient MEFs 'loaded' with recombinant HMGB1 proteins. Consistent with the role of HMGB1 in mediating the sensing of nucleic acids by the immune system, the addition of HMGB1 facilitated more transfer of B-DNA into endosomal vesicles positive for the early endosomal marker EEA1 in HMGB1-deficient MEFs than in HMGB1-competent wild-type cells (**Fig. 7a**). In contrast, B-DNA was located mainly around the plasma membrane, but the recruitment of B-DNA into endosomal vesicles was much lower in HMGB1-deficient MEFs transfected to express TIM-3 tagged with green fluorescent protein, followed by stimulation with HMGB1, than in wild-type MEFs (**Fig. 7a**), which suggested that TIM-3 interfered with HMGB1-dependent transfer of nucleic acids to the endosome. To further investigate whether endogenous TIM-3 had an inhibitory effect on the recruitment of nucleic acids to the endosome, we evaluated the endosomal localization of nucleic acids such as B-DNA or CpG-ODN in wild-type TIM-3$^+$ DCs or TIM-3-deficient TIM-3$^-$ DCs. A much greater portion of nucleic acids was localized to endosomal vesicles in TIM-3-deficient DCs than in wild-type TIM-3$^+$ DCs after stimulation with nucleic acids and HMGB1 (**Fig. 7b** and data not shown).

We next quantified B-DNA in total and EEA1$^+$ early endosomal vesicles in wild-type TIM-3$^+$ and TIM-3$^-$ DCs through the use of image-processing software[35]. The EEA1$^+$ endosomal vesicles of TIM-3$^+$ DCs had less B-DNA than did those of TIM-3$^-$ DCs, whereas total B-DNA was similar in both populations (**Fig. 7c**). Consistent with those findings, TIM-3 mainly localized together with HMGB1 in EEA1$^+$ endosomal vesicles in TIM-3$^+$ DCs after stimulation with HMGB1 (**Fig. 7d**).

To further substantiate the differences in the recruitment of DNA into endosomal vesicles in TIM-3$^+$ and TIM-3$^-$ cells, we purified endosomal vesicles by subcellular fractionation to measure the recruitment of DNA in wild-type TIM-3$^+$ or TIM-3$^-$ DCs. We confirmed that TIM-3$^+$ and TIM-3$^-$ DCs had similarly expression of the markers for early endosomes and late endosomes, as well as transfer-rin receptor (**Fig. 7e**). As expected, dot-blot analysis showed much less B-DNA in purified early or late endosomal vesicles from TIM-3$^+$ DCs than in those from TIM-3$^-$ DCs, whereas we detected more B-DNA in the heavy membrane fractions of TIM-3$^+$ DCs than in their TIM-3$^-$ counterparts. There was little difference between TIM-3$^+$ DCs and TIM-3$^-$ DCs in the amount of endocytosed DNA in the total and light plasma membrane fractions (**Fig. 7e**). Moreover, endosomal vesicles purified from HMGB1-stimulated TIM-3$^+$ DCs had less uptake of B-DNA than did those of HMGB1-stimulated TIM-3$^-$ DCs, as quantified by flow cytometry (**Supplementary Fig. 6**). Together these results demonstrated a role for TIM-3 in restraining the transport of nucleic acids to endosome, which is normally triggered by HMGB1.

We further examined the involvement of HMGB1 in TIM-3-mediated suppression through the use of HMGB1-deficient MEFs. Transfection of HMGB1-deficient MEFs to express TIM-3 had little inhibitory effect on cytokine production after stimulation with B-DNA, but the addition of recombinant HMGB1 protein restored the TIM-3-mediated suppression (**Fig. 7f**). Furthermore, treatment with neutralizing antibody to HMGB1 abrogated the nucleic acid–mediated responses elicited by blockade of TIM-3 in TIM-3$^+$ DCs to the amount in

cells treated with control immunoglobulin (**Fig. 7g**). Together these findings showed that TIM-3 may have negatively regulated HMGB1-mediated activation of the innate immune response to nucleic acids.

TIM-3 suppresses the antitumor effects of chemotherapy

Published studies have shown that some cytotoxic therapies may induce a form of immunogenic cell death in which the release of danger-associated molecules such as HMGB1 from dying tumor cells provides an endogenous adjuvant[36,37]. In addition, published evidence has shown that the immunogenicity of cancer vaccines is boosted by the simultaneous release of nucleic acids from dying tumors, which engenders the generation of protective antitumor immunity[38]. We therefore hypothesized that the TIM-3-mediated regulation of nucleic acid–sensing systems may modulate the antitumor immunity induced by chemotherapy-mediated 'immunogenic cell death'. To define the role of DC-derived TIM-3 in restraining cytotoxic agent–induced innate immune responses, we cultured TIM-3^+ DCs together with dying MC38 cells exposed a chemotherapeutic agent, in the presence of mAb to TIM-3. Treatment with mAb to TIM-3 resulted in more cytokine-encoding mRNA in TIM-3^+ DCs loaded with dying MC38 tumor cells treated with cisplatin (cis-diamminedichloroplatinum(II) (CDDP)) than did treatment with control immunoglobulin (**Fig. 8a**). The responses induced by mAb to TIM-3 were abrogated by the pretreatment of dying tumor cells with DNase and RNase (**Fig. 8a**), which indicated the involvement of nucleic acids. The responses triggered by treatment with supernatants of CDDP-treated MC38 cells, which contained free nucleic acids released from dying tumor cells, were also regulated through the nucleic acid–mediated innate sensing systems by TIM-3 (**Supplementary Fig. 7a**).

The kinase TBK1 serves as a critical regulator of nucleic acid–mediated innate immunity[7]. Consistent with the importance of TBK1 in this response, cytokine induction by dying tumors was suppressed in DCs deficient in both TBK1 and tumor-necrosis factor (TNF) relative to its induction in wild-type DCs or TNF-deficient DCs, and mAb to TIM-3 had little effect on IFN-β1 expression in DCs deficient in both TBK1 and TNF (**Fig. 8b**). These results indicated a critical contribution of TBK1 to these responses. Consistent with the role of TIM-3 in interfering with HMGB1-mediated nucleic acid–sensing pathways, blockade of TIM-3 in TIM-3^+ DCs cultured with CDDP-treated dying MC38 tumor cells did not result in more IFN-β in the presence of neutralizing antibody to HMGB1 (**Fig. 8c**).

In vivo treatment with mAb to TIM-3 had little additive effect on CDDP-induced antitumor activity against MC38 tumors in CD11c-DTR mice depleted of DCs (**Fig. 8d**). Thus, the *in vivo* antitumor effects elicited by the combination of TIM-3 blockade and chemotherapy resulted mainly from the suppression of endogenous DC activity. Notably, depletion of $CD11c^+$ cells alone substantially retarded the tumor growth elicited by treatment with CDDP (**Fig. 8d**), which indicated that TADCs served as the main suppressors of antitumor responses. Furthermore, the antitumor effects triggered by mAb to TIM-3 and CDDP were substantially impaired in CD11c-DTR mice not treated with diphtheria toxin by treatment with neutralizing antibody to IFN-IR and to IL-12 (**Supplementary Fig. 7b**), which suggested that type I interferon and IL-12 served as the main effectors of the execution of antitumor immunity by CDDP and mAb to TIM-3. Furthermore, CDDP was more effective against MC38 tumors in diphtheria toxin–treated TIM-3-deficient CD11c-DTR mice than in TIM-3-deficient CD11c-DTR mice not treated with diphtheria toxin (**Fig. 8e**), which indicated that TIM-3 on endogenous DCs served as a major repressor of the antitumor effects of chemotherapy. Thus, our results have indicated that DC-specific TIM-3 served as a negative regulator of chemotherapy-induced antitumor responses by circumventing the nucleic acid–mediated innate immune pathways (**Supplementary Fig. 8**).

DISCUSSION

We have shown here that tumor-infiltrating DCs suppressed antitumor immune responses through TIM-3-mediated negative regulation of innate immune responses to nucleic acids. DC-derived TIM-3 interacted with HMGB1 to suppress the transport of nucleic acids into endosomal vesicles, thus attenuating the antitumor efficacy of DNA vaccines and cytotoxic chemotherapy by antagonizing nucleic acid–sensing systems. Our findings have demonstrated an additional mechanism by which DC-derived TIM-3 serves as a unique repressor of antitumor responses by targeting nucleic acids required for antitumor responses mediated by PRRs. More generally, whether myeloid cell–specific TIM-3 has a role in restraining innate immune responses to viral infection must be evaluated.

The gene encoding TIM-3 underwent substantial upregulation and reached higher expression and earlier expression in DCs than in $CD8^+$ T cells in tumor microenvironments. Indeed, TIM-3 expression on $CD8^+$ T cells increased gradually at later time points of tumor growth, in agreement with studies showing that TIM-3 expression reflects the phenotype of exhausted $CD8^+$ T cells at the chronic phase of tumors[16,39]. Our findings also showed high expression of TIM-3 by tumor-infiltrating myeloid cells other than DCs, such as tumor-associated macrophages. Whether TIM-3 regulates innate immune responses in different ways depending on the myeloid cell type should be explored in future studies.

The interaction between galectin-9 and TIM-3 on antigen-presenting cells has a positive role in DC maturation and the cross-priming of tumor-specific T cells[15,23]. In contrast, TIM-3 on DCs has a protumorigenic role and ‘turns down’ nucleic acid–mediated innate immune responses via a galectin-9-independent but HMGB1-dependent mechanism. We speculate that DC-derived TIM-3 serves as a dual regulator of innate and adaptive immunity depending on the microenvironment. In tumor microenvironments, which are characterized by impaired induction of galectin-9 and high expression of HMGB1, TIM-3 on DCs may suppress innate immune responses by interfering with HMGB1-mediated stimulation of nucleic acid sensing, whereas TIM-3 maintains the anergic status of $CD8^+$ T cells in a tumor antigen–specific manner. These coordinated actions of TIM-3 on innate and adaptive responses may incapacitate efficient tumor immunosurveillance during all phases of tumorigenesis. In contrast, whereas DC-derived TIM-3 facilitates efficient containment of infectious agents by ‘preferentially’ interacting with galectin-9-enriched infectious microenvironments, TIM-3 on $CD8^+$ T cells has evolved to suppress antigen-specific responses and thus prevents excess tissue inflammation during the recovery phase after infection. In this context, the functional relevance of TIM-3 may be very different in cancer versus infection. This raises the possibility that proper concentrations of galectin-9 in tumor microenvironments may be crucial for controlling tumorigenesis and for overriding the TIM-3-mediated suppression of innate immune responses. Indeed, studies have shown that treatment with exogenous galectin-9 elicits antitumor responses by expanding and activating plasmacytoid DC-like macrophage and natural killer cell populations[40].

We also found that TIM-3 may have disrupted the recruitment of nucleic acids into the endosomal pathway by interfering with HMGB1 function, which led to impaired TLR- and cytosolic sensor–mediated innate immune responses. Although tumor cells are mainly composed of mutated or normal ‘self ’ nucleic acids, which are usually sequestered in the nucleus or mitochondria under physiological conditions, tumor microenvironments often acquire the ability to create an endogenous inflammatory milieu composed of damage-associated molecules such as HMGB proteins and uric acid[41]. Indeed, we found more HMGB1 in tumor tissues than their non-tumor counterparts. Such inflammatory signals could act together with tumor-derived nucleic acids to gain access to endosomal vesicles and

activate innate immune responses[30,34]. Thus, abundant expression of TIM-3 on TADCs may enable evasion of innate immune responses in the tumor microenvironment.

Despite our finding that TIM-3 suppressed the recruitment of nucleic acids to endosomes, several scenarios may be considered as additional mechanisms whereby TIM-3 interferes with the activation of nucleic acid–mediated responses by HMGB1. First, TIM-3 may affect HMGB1-mediated recognition of nucleic acids by modulating the activity of endosomal endonucleases such as TREX1 or FEN1, which are critical for mediating the degradation of host DNA[42,43]. Alternatively, TIM-3 may inhibit the activity of other HMGB1-binding partners, such as RAGE and TLR4, in endosomal vesicles[28,37]. In addition to its role in nucleic acid–mediated innate immune systems, TIM-3 may also regulate other functions of HMGB1, including gene transcription, oxidative stress and autophagy[29,44].

An additional finding of our study was that blockade of TIM-3 augmented the antitumor efficacy of anticancer cytotoxic agents in part by augmenting HMGB1-mediated nucleic acid–sensing systems. Our observations are consistent with published reports showing that tumor-derived nucleic acids act together with danger signals to activate cells of the innate immune response through the activation of PRR-mediated pathways[38]. As TIM-3 also serves as a receptor for phosphatidylserine for the engulfment of apoptotic cells, blockade of TIM-3 may also manipulate the phagocytotic pathway in DCs, thus modifying mechanisms for the recognition of dying tumor cells. Further investigation should determine the signaling cascades by which TIM-3 on DCs controls innate immune pathways during encounters with dying tumor cells.

Several lines of evidence have emphasized the role of certain cytotoxic drugs in triggering immunogenic cell death that results in the enhancement of host antitumor immunity to tumor cells through multiple pattern-recognition systems[36]. CDDP has been perceived as a ‘nonimmunogenic’ chemotherapeutic agent because it is unable to induce the endoplasmic reticulum stress responses mandatory for triggering antigen-specific T cell responses mediated by danger- associated molecular patterns[37,45]. Instead, CDDP may compromise the antitumor innate responses of DCs by acting together with TIM-3-dependent inhibitory pathways. Thus, our findings may have provided additional evidence that the therapeutic efficacy of even ‘nonimmunogenic’ chemotherapy can be induced by the targeting of negative regulatory mechanisms that restrain nucleic acid–mediated innate immune responses.

In summary, we have presented evidence that TIM-3 serves as a negative regulator of nucleic acid–dependent innate immune responses in tumor microenvironments. Given published findings showing that TIM-3 serves as a functional marker of leukemia stem cells[46,47], we propose that TIM-3 is a major sentinel that promotes tumor progression by manipulating multiple pathways to support tumorigenic microenvironments. The many facets of TIM-3 in tumor biology position pharmacological targeting of TIM-3 as a promising strategy for treating patients who are refractory to the anticancer modalities available at present.

ONLINE METHODS

Mice

C57BL/6, NOD-SCID and CD11c-DTR mice were from SCL, Charles River and Jackson Laboratory respectively. Mice deficient in both TBK1 and TNF were provided by S. Akira. TIM-3-deficient mice were generated and used as described[48]. All experiments were done according to a protocol approved by the animal care committees of Hokkaido University.

Samples from humans

The clinical protocols for this project were approved by the Institutional Review Board of Hokkaido University Hospital (10-0114). Tumor tissues and peripheral blood were obtained from patients with stage IV NSCLC, colon carcinoma, gastric carcinoma or neuroendocrine tumors after written informed consent was obtained. Cells were isolated by Ficoll-Hypaque density centrifugation and were further purified as $CD11c^+$ DCs from tumors and peripheral blood.

Tumor cells and MEFs

MC38, B16-F10 and 3LL tumor cells were from American Type Culture Collection. MEFs were isolated from wild-type and HMGB1-deficient mice.

TIM-3 expression

TIM-3 expression on $CD11c^{lo}B220^+PDCA1^+$ plasmacytoid DCs, $CD11c^{hi}$ conventional DCs, $F4/80^+CD11b^+$ macrophages, $CD45^-gp38^+$ stromal cells, tumor cells in tumor tissues, tumor-draining lymph nodes, distal lymph nodes or spleens obtained from tumor-bearing mice were analyzed by flow cytometry with mAb to mouse TIM-3 (RMT3-23; prepared in-house[26]). For primary tumor infiltrates obtained from patients with advanced cancer or in peripheral mononuclear cells, TIM-3 in $CD11c^+$ DCs was also assessed by flow cytometry with mAb to human TIM-3 (344823; R&D Systems). The *in vitro* induction of TIM-3 in BMDCs was examined 24 h after coculture or treatment with supernatants of tumors cells with mAb to VEGF-R2 (DC101; Calbiochem), mAb to IL-10 (JES5-16E3; BioLegend), TGF-β-receptor inhibitor SB52334 (R&D Systems), anti-galectin-9 (RG9-35), inhibitor of arginiase I ((S)-(2-boronoethyl)-L-cysteine; Sigma-Aldrich) or 1-methyltryptophan (Sigma-Aldrich).

Cytokine ELISA

For analysis of DC cytokine profiles, IFN-β, IFN-α, IL-6 and IL-12 in supernatants obtained from cultured cells were quantified by ELISA according to the manufacturer's instructions (BD Bioscience).

Quantification of cytokine mRNA

First, mRNA was isolated from cell lines, tumor-infiltrating DCs, tumor-draining lymph nodes or spleens after vaccination of tumor-bearing mice with plasmid DNA and treatment with mAb to TIM-3, or DCs from healthy donors or patients with NSCLC. Then, cytokine-encoding mRNA (IFN-β, IFN-α, IL-6 and IL-12) was quantified by real-time RT-PCR by SYBR Green Gene Expression Assay (Applied BioSystems).

In vivo antitumor effects of DNA adjuvants and mAb to TIM-3

Wild-type or NOD-SCID mice were injected subcutaneously in the flank with 1×10^5 B16-F10 melanoma cells, and intratumor injection of plasmid encoding human gp100, TRP-2 or control DNA, or CpG-ODN (10 μg/mouse; InvivoGen), in the presence of mAb RMT3-23 to TIM-3 (250 μg/mouse) or control immunoglobulin, were done on days 8, 10 and 12 after cell injection.

In vivo antitumor effects of DNA adjuvants in CD11c-DTR mice

CD11c-DTR mice were left untreated or treated with diphtheria toxin (4 ng per gram body weight, every 2 d from day 2 to day 22) for depletion of $CD11c^+$ cells. B16-F10 or MC38 tumor cells (1×10^5 cells per mouse) were injected into CD11c-DTR mice and mice were treated with control plasmid DNA (50 μg per mouse) and/or mAb RMT3-23 to TIM-3 (250

μg per mouse) in the presence or absence of antibody to the receptor for type I IFN-α2 (100 μg/mouse; MMHAR-2; BioLegend) and anti-IL-12p40 (250 μg per mouse; C17.8; eBioscience) on days 2, 5 and 8 after tumor inoculation.

Generation of mixed–bone marrow chimeras

The mixed–bone marrow chimeras were generated as described[49]. Bone marrow cells isolated from wild-type or TIM-3-deficient mice were mixed with those from CD11c -DTR mice at a ratio of 1:1. Bone marrow cells (1×10^6 cells per mouse) were transferred intravenously into lethally irradiated mice (15 Gy per mouse). The efficacy of donor-cell reconstitution was evaluated by the identification of $CD11c^{hi}$ major histocompatibility complex class II–positive populations in peripheral blood 4 weeks after the procedure.

TIM-3–HMGB1 interaction

Fusion proteins of Fc and wild-type TIM-3, Q62A mutant TIM-3 or Flt3L were used to coat plastic plates, which were then loaded with biotin-labeled HMGB1 at various concentrations. The binding of biotin-labeled HMGB1 to each fusion protein was measured by colorimetric analysis (absorbance at 450 nm). In some studies, mAb to TIM-3 was added with the HMGB-1 protein.

Generation of recombinant HMGB1 protein

A series of expression vectors with various deletions of HMGB1 (pET28b-HMGB1-Full, pET28b-HMGB1-ΔC-box, pIVEX2.4-HMGB1-ΔA-box, pIVEX2.4-HMGB1-ΔBΔC-box, and pET28b-GST) were introduced into BL21 competent cells, then proteins were induced and purified as described[50].

Immunofluorescence microscopy

BMDCs and MEFs were stimulated with biotin-labeled HMGB1 and X rhodamine–labeled B-DNA. After cells were fixed, early endosomes were probed by Alexa Fluor 488–labeled mAb to EEA1 (C45B10; Cell Signaling Technology), and internalized HMGB1 was probed by streptavidin–Brilliant Violet 421. Images were obtained with an FV-1000D laser confocal microscope (Olympus). Visualized DNA in endosomes was quantified with MetaMorph software (Universal Imaging). Confocal sections (with a z-step of 0.42 μm) were acquired from the bottom to the top of the cells, and all sections were projected on one image plane. $B\text{-}DNA^+$ or $EEA1^+$ vesicles were extracted as regions with the ‘granularity’ module and those images were overlaid on the original B-DNA images, followed by quantification with the ‘measure region’ function.

Subcellular fractionation and detection of B-DNA

$TIM\text{-}3^+$ or $TIM\text{-}3^-$ DCs were incubated for 90 min with biotin-labeled B-DNA. Cells were homogenized with HB^+ (250 mM sucrose, 3 mM imidazole pH 7.4, 1 mM EDTA, 30 mM cycloheximide), and the postnuclear supernatants were subjected to sucrose-gradient ultracentrifugation at 150,000*g* for 1 h with step gradients of 40.6%, 35%, 25%, and 8%. After centrifugation, interfaces were collected (8%/25% late endosome; 25%/35% early endosome), and analyzed by immunoblot and DNA dot blot. For the preparation of heavy and light plasma membrane fraction, postnuclear supernatants were centrifuged for 30 min at 100,000*g* in 30% percoll gradient. For the detection of biotin-labeled B-DNA, each fraction was dotted onto a positively charged nylon membrane, which was probed with streptavidin–horseradish peroxidase.

Evaluation of chemotherapy-mediated antitumor responses

For *in vivo* tumor experiments, CD11c-DTR mice or bone marrow chimeras were challenged subcutaneously in the flank with MC38 cells (1×10^5), and CDDP (10 mg/kg), mAb RMT3-23 to TIM-3 (250 μg/mouse), anti-IFN-IR (100 μg per mouse; MMHAR-2; BioLegend) or anti-IL-12p40 (250 μg per mouse; C17.8; eBioscience) was injected intraperitoneally on days 8, 10 and 12. For *in vitro* assays, TIM-3^+ BMDCs were cultured together with apoptotic tumor cells pretreated with DNase and RNase (10 μg/ml; Invitrogen) in the presence of mAb to TIM-3, anti-HMGB1 (326052233; Shino-Test) or control immunoglobulin (731705; Beckman-Coulter), and cytokine-encoding mRNA was evaluated by RT-PCR.

Statistical analysis

A paired Student's *t*-test was used for statistical analyses, and a *P* value of less than 0.05 was considered statistically significant.

Supplementary Material

Refer to Web version on PubMed Central for supplementary material.

Acknowledgments

We thank M. Bianchi (San Raffaele University) for MEFs deficient in HMGB1 and HMGB2; O. Takeuchi and S. Akira (Osaka University) for mice deficient in both TBK1 and TNF; J. Wolchok (Memorial Sloan-Kettering Cancer Center) for plasmids encoding gp100 and TRP-2; G. Dranoff for comments on the manuscript; and T. Yamashina for assistance with animal care. Supported by the Ministry of Education, Culture, Sports, Science and Technology of Japan (H. Yagita and M.J.), the National Cancer Center Research and Development Fund (H.Ya.), the Institute for Genetic Medicine of Hokkaido University (M.J., M.H. and H.Ya.), the Takeda Science Foundation (M.J.), the Sumitomo Foundation (M.J.), Terumo Life Science Foundation (M.J.), Senshin Medical Research Foundation (M.J.) and Japan Leukemia Research Foundation (M.J.).

References

1. Hanahan D, Weinberg RA. Hallmarks of cancer: the next generation. Cell. 2011; 144:646–674. [PubMed: 21376230]
2. Schreiber RD, Old LJ, Smyth MJ. Cancer immunoediting: integrating immunity's roles in cancer suppression and promotion. Science. 2011; 331:1565–1570. [PubMed: 21436444]
3. Bindea G, Mlecnik B, Fridman WH, Pages F, Galon J. Natural immunity to cancer in humans. Curr. Opin. Immunol. 2010; 22:215–222. [PubMed: 20207124]
4. Dougan M, Dranoff G. Immune therapy for cancer. Annu. Rev. Immunol. 2009; 27:83–117. [PubMed: 19007331]
5. Rabinovich GA, Gabrilovich D, Sotomayor EM. Immunosuppressive strategies that are mediated by tumor cells. Annu. Rev. Immunol. 2007; 25:267–296. [PubMed: 17134371]
6. Drake CG, Jaffee E, Pardoll DM. Mechanisms of immune evasion by tumors. Adv. Immunol. 2006; 90:51–81. [PubMed: 16730261]
7. Takeuchi O, Akira S. Pattern recognition receptors and inflammation. Cell. 2010; 140:805–820. [PubMed: 20303872]
8. Steinman RM, Banchereau J. Taking dendritic cells into medicine. Nature. 2007; 449:419–426. [PubMed: 17898760]
9. Peng G, et al. Toll-like receptor 8-mediated reversal of $CD4^+$ regulatory T cell function. Science. 2005; 309:1380–1384. [PubMed: 16123302]
10. Poeck H, et al. 5′-Triphosphate-siRNA: turning gene silencing and Rig-I activation against melanoma. Nat. Med. 2008; 14:1256–1263. [PubMed: 18978796]

11. Besch R, et al. Proapoptotic signaling induced by RIG-I and MDA-5 results in type I interferon-independent apoptosis in human melanoma cells. J. Clin. Invest. 2009; 119:2399–2411. [PubMed: 19620789]
12. Kuchroo VK, Dardalhon V, Xiao S, Anderson AC. New roles for TIM family members in immune regulation. Nat. Rev. Immunol. 2008; 8:577–580. [PubMed: 18617884]
13. Sánchez-Fueyo A, et al. Tim-3 inhibits T helper type 1-mediated auto- and alloimmune responses and promotes immunological tolerance. Nat. Immunol. 2003; 4:1093–1101. [PubMed: 14556005]
14. Zhu C, et al. The Tim-3 ligand galectin-9 negatively regulates T helper type 1 immunity. Nat. Immunol. 2005; 6:1245–1252. [PubMed: 16286920]
15. Anderson AC, et al. Promotion of tissue inflammation by the immune receptor Tim-3 expressed on innate immune cells. Science. 2007; 318:1141–1143. [PubMed: 18006747]
16. Zhou Q, et al. Coexpression of Tim-3 and PD-1 identifies a $CD8^+$ T-cell exhaustion phenotype in mice with disseminated acute myelogenous leukemia. Blood. 2011; 117:4501–4510. [PubMed: 21385853]
17. Munn DH, et al. Potential regulatory function of human dendritic cells expressing indoleamine 2,3-dioxygenase. Science. 2002; 297:1867–1870. [PubMed: 12228717]
18. Norian LA, et al. Tumor-infiltrating regulatory dendritic cells inhibit $CD8^+$ T cell function via L-arginine metabolism. Cancer Res. 2009; 69:3086–3094. [PubMed: 19293186]
19. Gabrilovich DI, et al. Production of vascular endothelial growth factor by human tumors inhibits the functional maturation of dendritic cells. Nat. Med. 1996; 2:1096–1103. [PubMed: 8837607]
20. Bowne WB, et al. Coupling and uncoupling of tumor immunity and autoimmunity. J. Exp. Med. 1999; 190:1717–1722. [PubMed: 10587362]
21. Ngiow SF, et al. Anti-TIM3 antibody promotes T cell IFN-γ-mediated antitumor immunity and suppresses established tumors. Cancer Res. 2011; 71:3540–3551. [PubMed: 21430066]
22. Drobits B, et al. Imiquimod clears tumors in mice independent of adaptive immunity by converting pDCs into tumor-killing effector cells. J. Clin. Invest. 2012; 122:575–585. [PubMed: 22251703]
23. Nagahara K, et al. Galectin-9 increases $Tim\text{-}3^+$ dendritic cells and $CD8^+$ T cells and enhances antitumor immunity via galectin-9-Tim-3 interactions. J. Immunol. 2008; 181:7660–7669. [PubMed: 19017954]
24. Jayaraman P, et al. Tim3 binding to galectin-9 stimulates antimicrobial immunity. J. Exp. Med. 2010; 207:2343–2354. [PubMed: 20937702]
25. Dardalhon V, et al. Tim-3/galectin-9 pathway: regulation of Th1 immunity through promotion of $CD11b^+Ly\text{-}6G^+$ myeloid cells. J. Immunol. 2010; 185:1383–1392. [PubMed: 20574007]
26. Nakayama M, et al. Tim-3 mediates phagocytosis of apoptotic cells and cross-presentation. Blood. 2009; 113:3821–3830. [PubMed: 19224762]
27. DeKruyff RH, et al. T cell/transmembrane, Ig, and mucin-3 allelic variants differentially recognize phosphatidylserine and mediate phagocytosis of apoptotic cells. J. Immunol. 2010; 184:1918–1930. [PubMed: 20083673]
28. Ablasser A, et al. RIG-I-dependent sensing of poly(dA:dT) through the induction of an RNA polymerase III-transcribed RNA intermediate. Nat. Immunol. 2009; 10:1065–1072. [PubMed: 19609254]
29. Sims GP, Rowe DC, Rietdijk ST, Herbst R, Coyle AJ. HMGB1 and RAGE in inflammation and cancer. Annu. Rev. Immunol. 2010; 28:367–388. [PubMed: 20192808]
30. Tian J, et al. Toll-like receptor 9-dependent activation by DNA-containing immune complexes is mediated by HMGB1 and RAGE. Nat. Immunol. 2007; 8:487–496. [PubMed: 17417641]
31. Yanai H, et al. HMGB proteins function as universal sentinels for nucleic-acid-mediated innate immune responses. Nature. 2009; 462:99–103. [PubMed: 19890330]
32. Cao E, et al. T cell immunoglobulin mucin-3 crystal structure reveals a galectin-9-independent ligand-binding surface. Immunity. 2007; 26:311–321. [PubMed: 17363302]
33. Santiago C, et al. Structures of T cell immunoglobulin mucin protein 4 show a metal-Ion-dependent ligand binding site where phosphatidylserine binds. Immunity. 2007; 27:941–951. [PubMed: 18083575]

34. Blasius AL, Beutler B. Intracellular toll-like receptors. Immunity. 2010; 32:305–315. [PubMed: 20346772]
35. Fujioka Y, et al. The Ras-PI3K signaling pathways is involved in clathrin-independnet endocytosis and the internalization of influenza viruses. PLoS ONE. 2011; 6:e16324. [PubMed: 21283725]
36. Green DR, Ferguson T, Zitvogel L, Kroemer G. Immunogenic and tolerogenic cell death. Nat. Rev. Immunol. 2009; 9:353–363. [PubMed: 19365408]
37. Apetoh L, et al. Toll-like receptor 4-dependent contribution of the immune system to anticancer chemotherapy and radiotherapy. Nat. Med. 2007; 13:1050–1059. [PubMed: 17704786]
38. Lin Y, et al. Effective post-transplant antitumor immunity is associated with TLR-stimulating nucleic acid-immunoglobulin complexes in humans. J. Clin. Invest. 2011; 121:1574–1584. [PubMed: 21403403]
39. Jones RB, et al. Tim-3 expression defines a novel population of dysfunctional T cells with highly elevated frequencies in progressive HIV-1 infection. J. Exp. Med. 2008; 205:2763–2779. [PubMed: 19001139]
40. Nobumoto A, et al. Galectin-9 expands unique macrophages exhibiting plasmacytoid dendritic cell-like macrophages that activate NK cells in tumor-bearing mice. Clin. Immunol. 2009; 130:322–330. [PubMed: 18974023]
41. Grivennikov SI, Greten FR, Karin M. Immunity, inflammation, and cancer. Cell. 2010; 140:883–899. [PubMed: 20303878]
42. Stetson DB, Ko JS, Heidmann T, Medzhitov R. Trex1 prevents cell-intrinsic initiation of autoimmunity. Cell. 2008; 134:587–598. [PubMed: 18724932]
43. Zheng L, et al. Fen1 mutations results in autoimmunity, chronic inflammation and cancers. Nat. Med. 2007; 13:812–819. [PubMed: 17589521]
44. Anderson U, Tracy KJ. HMGB1 in a therapeutic target for sterile inflammation and infection. Annu. Rev. Immunol. 2011; 29:139–162. [PubMed: 21219181]
45. Michaud M, et al. Autophagy-dependent anticancer immune responses induced by chemotherapeutic agents in mice. Science. 2011; 334:1573–1577. [PubMed: 22174255]
46. Kikushige Y, et al. TIM-3 is a promising target to selectively kill acute myeloid leukemia stem cells. Cell Stem Cell. 2010; 7:708–717. [PubMed: 21112565]
47. Jan M, et al. Prospective separation of normal and leukemic stem cells based on differential expression of TIM3, a human acute myeloid leukemia stem cell marker. Proc. Natl. Acad. Sci. USA. 2011; 108:5009–5014. [PubMed: 21383193]
48. Sabatos CA, et al. Interaction of Tim-3 and Tim-3 ligand regulates T helper type 1 responses and induction of peripheral tolerance. Nat. Immunol. 2003; 4:1102–1110. [PubMed: 14556006]
49. Kinnebrew MA, et al. Interleukin 23 production by intestinal $CD103^{+}$ $CD11b^{+}$ dendritic cells in response to bacterial flagellin enhances mucosal innate immune defense. Immunity. 2012; 36:276–287. [PubMed: 22306017]
50. Najima Y, et al. High mobility group protein-B1 interacts with sterol regulatory element-binding proteins to enhance their DNA binding. J. Biol. Chem. 2005; 280:27523–27532. [PubMed: 16040616]

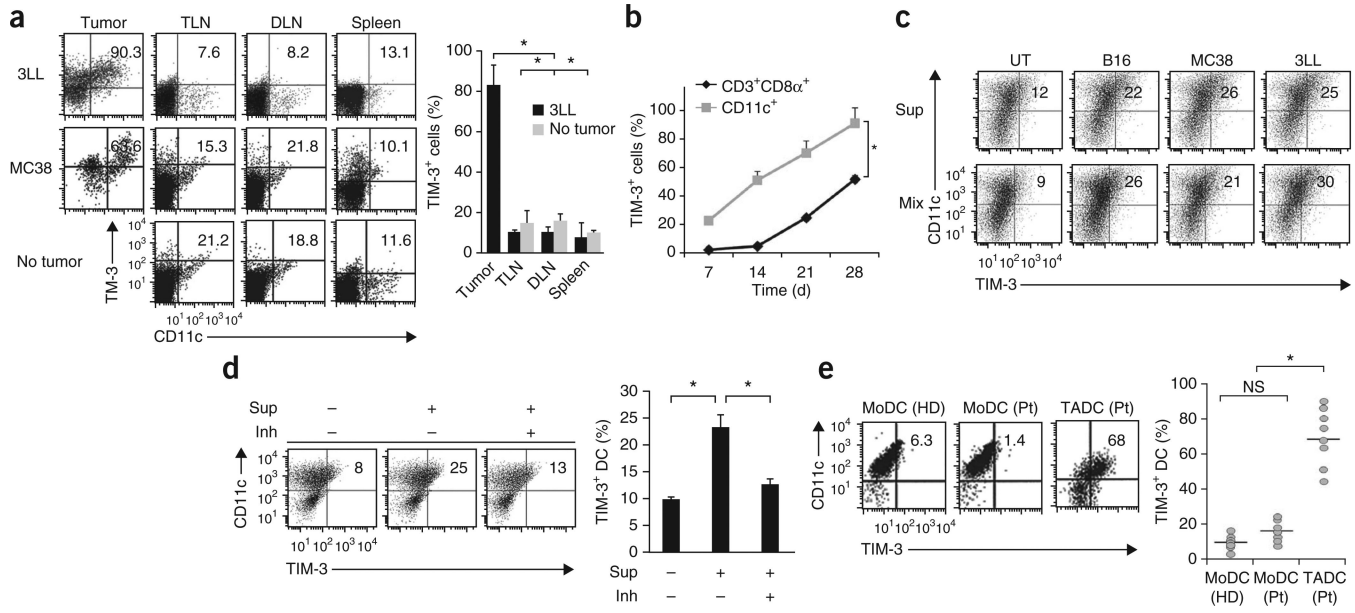

Figure 1.

Expression of TIM-3 on TADCs. (**a**) TIM-3 expression by DCs from established tumors (Tumor), tumor-draining lymph nodes (TLN), distal lymph nodes (DLN) or spleens of mice bearing 3LL or MC38 tumors at 28 d after tumor inoculation, and from tumor-free mice (No tumor; control), analyzed by flow cytometry (left). Numbers in top right quadrants indicate percent TIM-3$^+$CD11c$^+$ cells. Right, TIM-3$^+$ cells among CD11c$^+$ cells isolated from mice bearing 3LL tumors or no tumors (average). (**b**) Longitudinal analysis of TIM-3-expressing CD11c$^+$ DCs or CD3$^+$CD8$^+$ T cells (Cd3$^+$CD8α$^+$) after inoculation of 3LL tumors. (**c**) TIM-3 expression by BMDCs left untreated (UT) or treated for 48 h with supernatants of B16, MC38 or 3LL tumor cells (20% in total medium; Sup) or cultured for 48 h together with those tumor cells (Mix), evaluated by flow cytometry (numbers in plots as in **a**). (**d**) TIM-3 expression on BMDCs left untreated (Sup –) or treated for 48 h with supernatants of 3LL cell cultures (Sup +) left untreated (Inh –) or treated with anti-VEGF-R2, anti-IL-10 and inhibitor of arginase I (Inh +), evaluated by flow cytometry (left; numbers in plots as in **a**). Right, frequency of TIM-3$^+$CD11c$^+$ DCs. (**e**) TIM-3 expression on DCs differentiated from peripheral blood monocytes (MoDCs) from healthy donors (HD; $n = 7$) or patients with cancer (Pt; $n = 7$), and TADCs from those same patients ($n = 9$), evaluated by flow cytometry (left; numbers in plots as in **a**). Right, frequency of TIM-3$^+$CD11c$^+$ DCs; each symbol represents an individual donor, and small horizontal lines indicate the mean. NS, not significant. *$P < 0.05$ (paired Student's t-test). Data are representative of four experiments (**a–d**; error bars (**a,b,d**), s.e.m.) or three experiments (**e**).

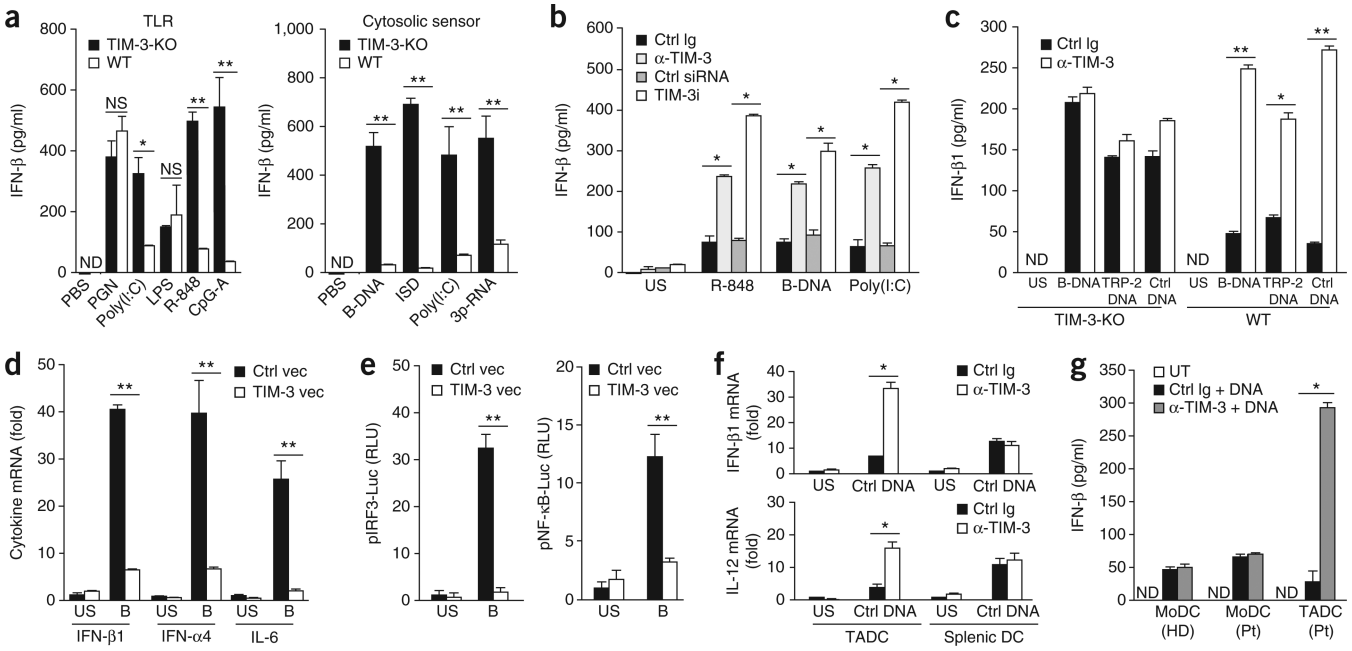

Figure 2.

TIM-3 suppresses innate responses to nucleic acids. (**a**) Enzyme-linked immunosorbent assay (ELISA) of IFN-β in wild-type TIM-3$^+$ BMDCs (WT) or TIM-3-deficient TIM-3$^-$ BMDCs (TIM-3-KO) stimulated with PBS or various TLR ligands (left: peptidoglycan (PGN), poly(I:C), lipopolysaccharide (LPS), R-848 or CpG ODN1585 (CpG-A)) or agonists of cytosolic sensors (right: B-DNA, interferon-stimulatory DNA (ISD), poly(I:C) or triphosphate RNA (3p-RNA)). (b) ELISA of IFN-β1 in wild-type TIM-3$^+$ DCs treated with control immunoglobulin (Ctrl Ig), mAb to TIM-3 (α-TIM-3), control small interfering RNA (Ctrl siRNA) or small interfering RNA specific for TIM-3 (TIM-3i), followed by no stimulation (unstimulated (US)) or stimulation for 8 h with PBS, R-848, B-DNA or poly(I:C). (**c**) ELISA of IFN-β1 in wild-type TIM-3$^+$ or TIM-3-deficient TIM-3$^-$ BMDCs pretreated with control immunoglobulin or mAb to TIM-3, followed by no stimulation or stimulation for 12 h with B-DNA, plasmid encoding TRP-2 (TRP-2 DNA) or plasmid without insert (Ctrl DNA). (**d**) Quantification of IFN-β1, IFN-α4 and IL-6 mRNA in MEFs transfected for 24 h with control vector (Ctrl vec) or vector encoding TIM-3 (TIM-3 vec), followed by no stimulation or stimulation for 8 h with B-DNA (B); results are presented relative to the expression of *Actb* (reference gene encoding β-actin). (**e**) Luciferase activity in lysates of HEK293T cells transfected and treated as in **d**, assessing the activity of IRF3 (pIRF3-Luc) or NF-κB (pNF-κB-Luc); results are presented in relative light units (RLU) relative to the activity of renilla luciferase. (**f**) RT-PCR quantification of IFN-β1 and IL-12 mRNA in TADCs and splenic DCs isolated from tumor-bearing mice treated with control immunoglobulin or mAb to TIM-3, followed by no stimulation or stimulation for 8 h with plasmid DNA (Ctrl DNA); results are presented relative to *Actb* expression. (**g**) ELISA of IFN-β in DCs differentiated from peripheral blood monocytes from healthy donors or patients with NSCLC, and TADCs from those same patients, left untreated or pretreated with control immunoglobulin or mAb to TIM-3, followed by stimulation with B-DNA (+ DNA). *$P < 0.05$ and **$P < 0.01$ (paired Student's *t*-test). Data are representative of five experiments (**a**), four experiments (**b,c**) or three experiments (**d–g**; error bars, s.e.m.).

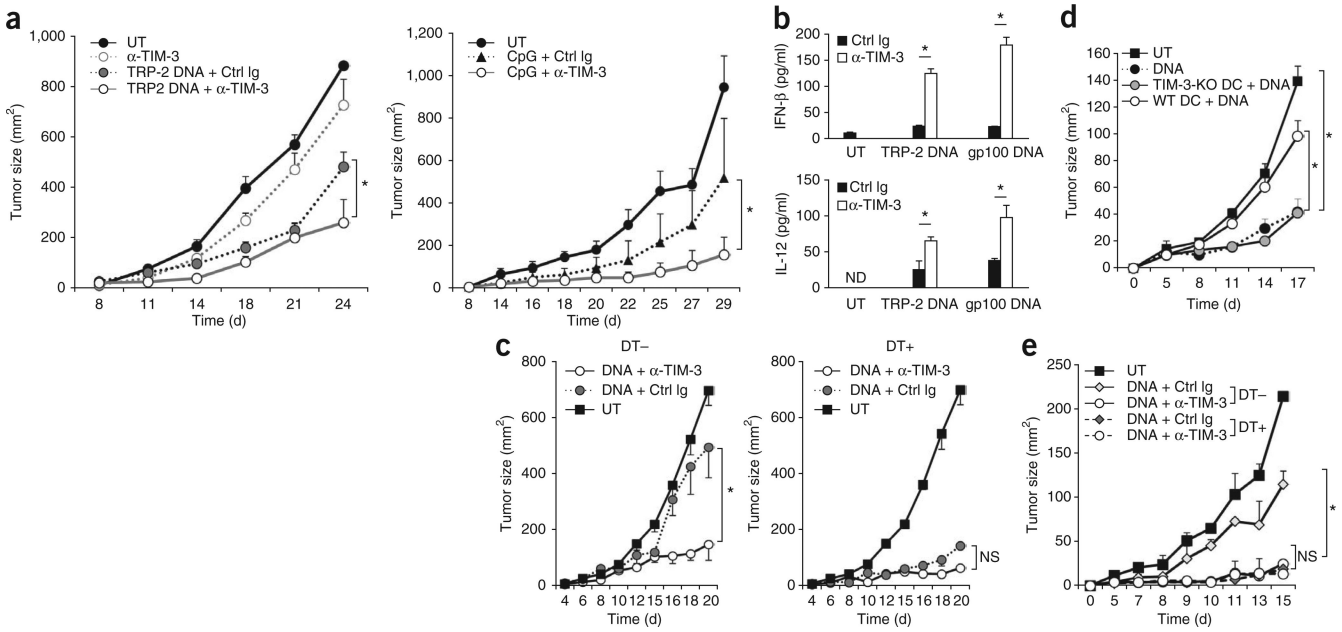

Figure 3.

TIM-3 impedes the *in vivo* antitumor activities of DNA. (**a**) Tumor growth in wild-type C57BL/6 mice ($n = 4$ per group) left untreated or inoculated subcutaneously in the flank with B16-F10 melanoma cells, then given intratumoral injection of mAb to TIM-3 alone (left) or of plasmid encoding mouse TRP-2 (TRP-2 DNA; left) or CpG-ODN (CpG; right) in the presence of control immunoglobulin or mAb to TIM-3 (key). (**b**) ELISA of IFN-β and IL-12 in lysates of B16-F10 tumors isolated from untreated mice or mice treated with plasmid encoding TRP-2 or gp100 in the presence of control immunoglobulin or mAb to TIM-3 (key). (**c**) Tumor growth in CD11c-DTR mice given no treatment with diphtheria toxin (DT–) or treated with diphtheria toxin (DT+), then left untreated or inoculated subcutaneously with B16-F10 melanoma cells (1×10^5 cells per mouse) along with control plasmid DNA in the presence of mAb to TIM-3 or isotype-matched control immunoglobulin. (**d**) Tumor growth in diphtheria toxin–treated CD11c-DTR mice ($n = 5$ per group) given no treatment (UT), control plasmid alone (DNA) or adoptive transfer of DCs derived from wild-type or TIM-3-deficient bone marrow, along with intratumoral injection of control plasmid DNA into established B16-F10 tumors. (**e**) Tumor growth in chimeras reconstituted with a mixture of bone marrow cells from TIM-3-deficient mice and CD11c-DTR mice given no treatment with diphtheria toxin or treated with diphtheria toxin 2 d before inoculation with B16-F10 tumor cells (1×10^5 cells per mouse), then left untreated (UT) or treated 8, 10 and 12 d later with control plasmid DNA in the presence of isotype-matched control immunoglobulin or mAb to TIM-3 after tumor inoculation. $*P < 0.05$ (paired Student's *t*-test). Data are representative of four experiments (**a**), three experiments (**b,c**), two independent experiments (**d**) or two experiments (**e**; error bars, s.e.m.).

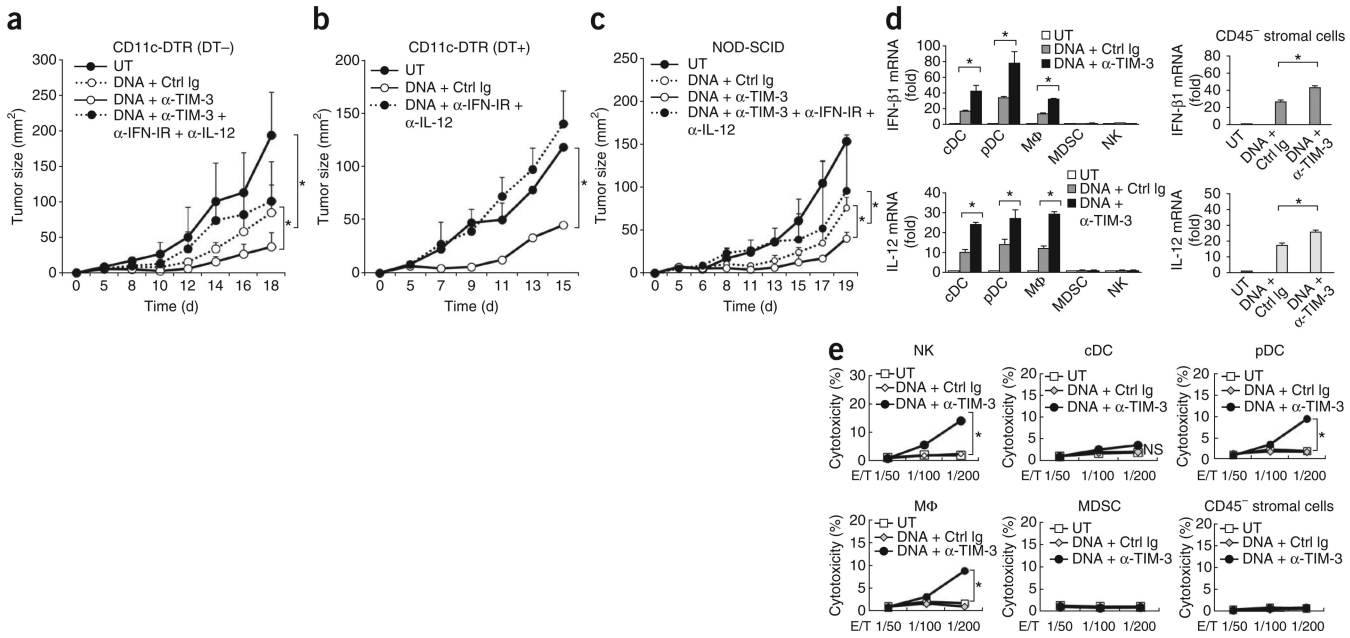

Figure 4.

Type I interferon and IL-12 mediate anti-TIM-3-mediated antitumor responses. (**a–c**) Tumor growth in CD11c-DTR mice given no treatment with diphtheria toxin (**a**) or treated with diphtheria toxin (**b**), and in NOD-SCID mice (**c**), left untreated (control) or inoculated subcutaneously with B16-F10 cells (1×10^5 cells per mouse) along with intratumoral injection of control plasmid DNA in the presence of isotype-matched control immunoglobulin or mAb to TIM-3, alone or with neutralizing anti-IFN-IR and anti-IL-12p40. (**d**) RT-PCR quantification of IFN-β1 and IL-12 mRNA in conventional DCs (cDC), plasmacytoid DCs (pDC), macrophages (MΦ), myeloid-derived suppressor cells (MDSC), natural killer cells (NK; left) or stromal cells isolated from B16 tumors grown in NOD-SCID mice (right), left untreated or treated with control plasmid DNA plus isotype-matched control immunoglobulin or mAb to TIM-3; results are presented relative to *Actb* expression. (**e**) Cytotoxicity of the cells in **d** (effector cells; E) cultured together for 6 h with B16 cells (target cells; T) at various ratios (E/T), assessed by lactate dehydrogenase–release assay. $*P < 0.05$ (paired Student's *t*-test). Data are representative of three experiments (**a,c–e**) or four experiments (**b**; error bars, s.e.m.).

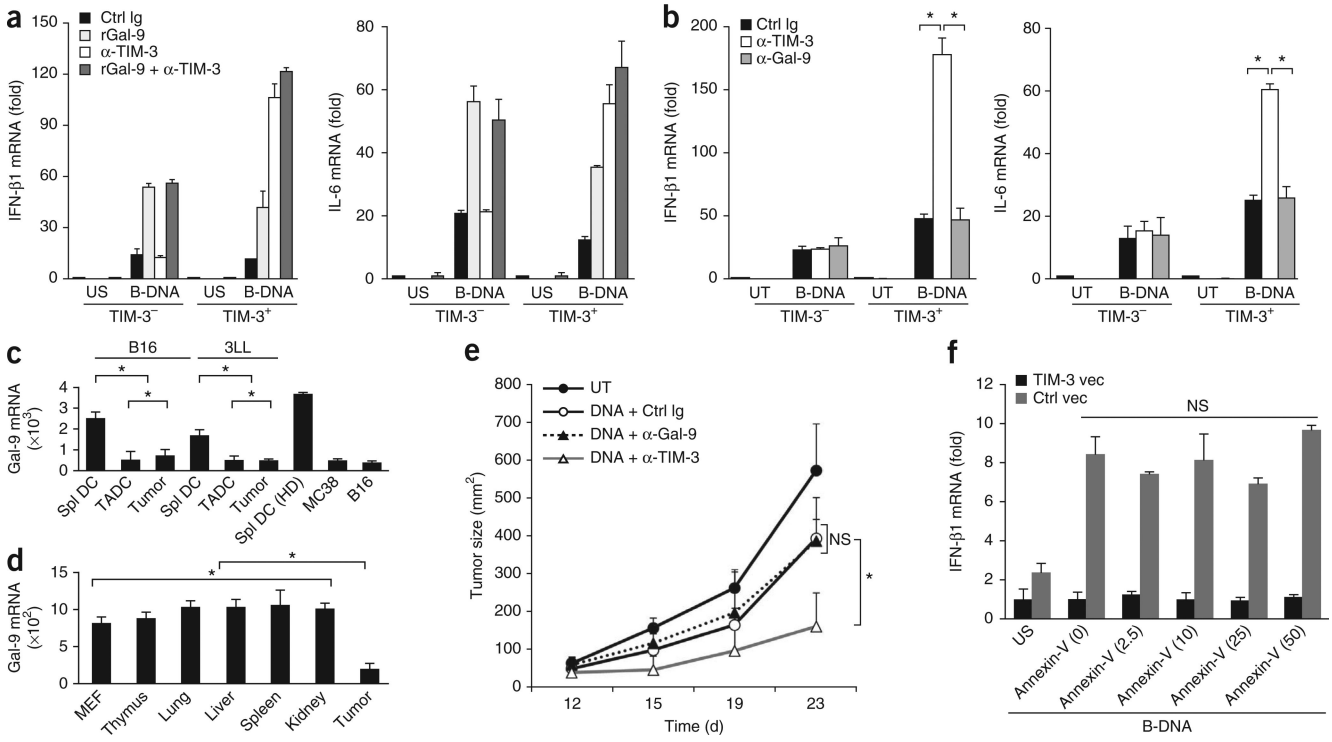

Figure 5.

TIM-3 regulates innate responses by a galectin-9-independent mechanism. (**a**) RT-PCR analysis of IFN-β1 and IL-6 mRNA in wild-type TIM-3$^+$ and TIM-3$^-$ BMDCs pretreated with isotype-matched control immunoglobulin, recombinant galectin-9 (rGal-9) and/or mAb to TIM-3 (key), followed by no stimulation or stimulation for 8 h with B-DNA; results are presented relative to *Actb* expression. (**b**) RT-PCR quantification of IFN-β1 and IL-6 mRNA in TIM-3$^+$ and TIM-3$^-$ BMDCs left untreated or treated for 24 h with B-DNA in the presence of isotype-matched control immunoglobulin, mAb to TIM-3 or mAb to galectin-9; results are presented relative to *Actb* expression. (**c**) RT-PCR quantification of galectin-9 (Gal-9) mRNA in splenic DCs (Spl DC), TADCs and tumor cells isolated from established B16 or 3LL tumors, splenic DCs from non-tumor-bearing mice (HD) and MC38 or 3LL tumor cells cultured *in vitro*; results are presented relative to *Actb* expression. (**d**) RT-PCR quantification of galectin-9 mRNA in MEFs, normal tissues (thymus, lung, liver, spleen and kidney) from tumor-bearing mice, and B16 tumors (Tumor); results are presented relative to expression of *Gapdh* (reference gene encoding glyceraldehyde phosphate dehydrogenase). (**e**) Tumor growth in C57BL/6 mice ($n = 4$ per group) left untreated or inoculated subcutaneously with B16-F10 melanoma cells (1×10^5 cells per mouse) and given intratumoral injection of control plasmid DNA in the presence of isotype-matched control immunoglobulin or mAb to galectin-9 or TIM-3. (f) RT-PCR analysis of IFN-β1 mRNA in MEFs transfected for 24 h with vector encoding TIM-3 or control vector, then left unstimulated or stimulated with B-DNA in the presence of various concentrations of recombinant annexin V (horizontal axis; in ng/ml). *$P < 0.05$ (paired Student's *t*-test). Data are representative of three experiments (**a–e**) or two experiments (**f**; error bars, s.e.m.).

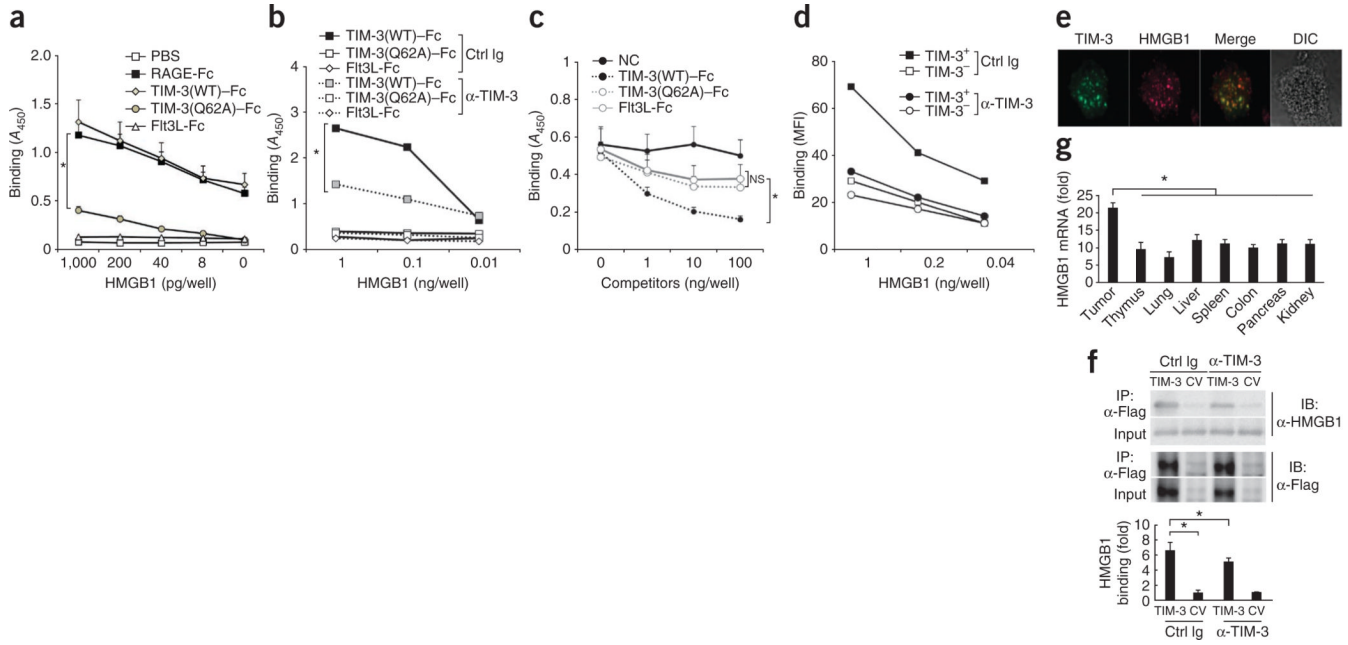

Figure 6.

TIM-3 serves as a putative receptor for HMGB1. (**a**) Binding of biotin-labeled recombinant HMGB1 (concentration, horizontal axis) to plastic plates coated with PBS or fusions of Fc and RAGE (RAGE-Fc), wild-type TIM-3 (TIM-3(WT)–Fc), mutant TIM-3 (TIM-3(Q62A)–Fc) or the cytokine Flt3L (Flt3L-Fc), measured by colorimetric analysis and presented as absorbance at 450 nm (A_{450}). (**b**) Binding of HMGB1 as in **a** in the presence of control immunoglobulin or mAb to TIM-3. (**c**) Binding of biotin-labeled B-DNA to plastic plates coated with HMGB1 in the absence (NC) or presence of TIM-3(WT)–Fc, TIM-3(Q62A)–Fc or Flt3L-Fc as cold competitors (concentrations, horizontal axis), measured and presented as in **a**. (**d**) Binding of biotin-labeled HMGB1 (concentration, horizontal axis) to wild-type TIM3$^+$ or TIM-3$^-$ BMDCs during culture with control immunoglobulin or mAb to TIM-3, analyzed by flow cytometry and are presented as mean fluorescence intensity (MFI). (**e**) Confocal microscopy of TIM-3 (green) in TIM-3$^+$ DCs loaded with recombinant HMGB1 (red). DIC, differential interference contrast. Original magnification, ×1,000. (**f**) Immunoassay (top) of lysates of MEFs transfected with vector encoding Flag-tagged TIM-3 or control vector (CV) and stimulated for 30 min with HMGB1 in the presence of control immunoglobulin or mAb to TIM-3, followed by immunoprecipitation (IP) with mAb M2 to the Flag tag and immunoblot analysis with anti-HMGB1 or anti-Flag. Bottom, band intensity of HMGB1–TIM-3 in MEFs transfected with TIM-3 relative to that in MEFs transfected with control vector (below). (**g**) RT-PCR quantification of HMGB1 mRNA in B16-F10 tumors and normal tissues; results are presented relative to *Actb* expression. *$P <$ 0.05 (paired Student's *t*-test). Data are representative of five experiments (**a,f**), four experiments (**b,c**) or three experiments (**d,e,g**; error bars (**a,c,d,f,g**), s.e.m.).

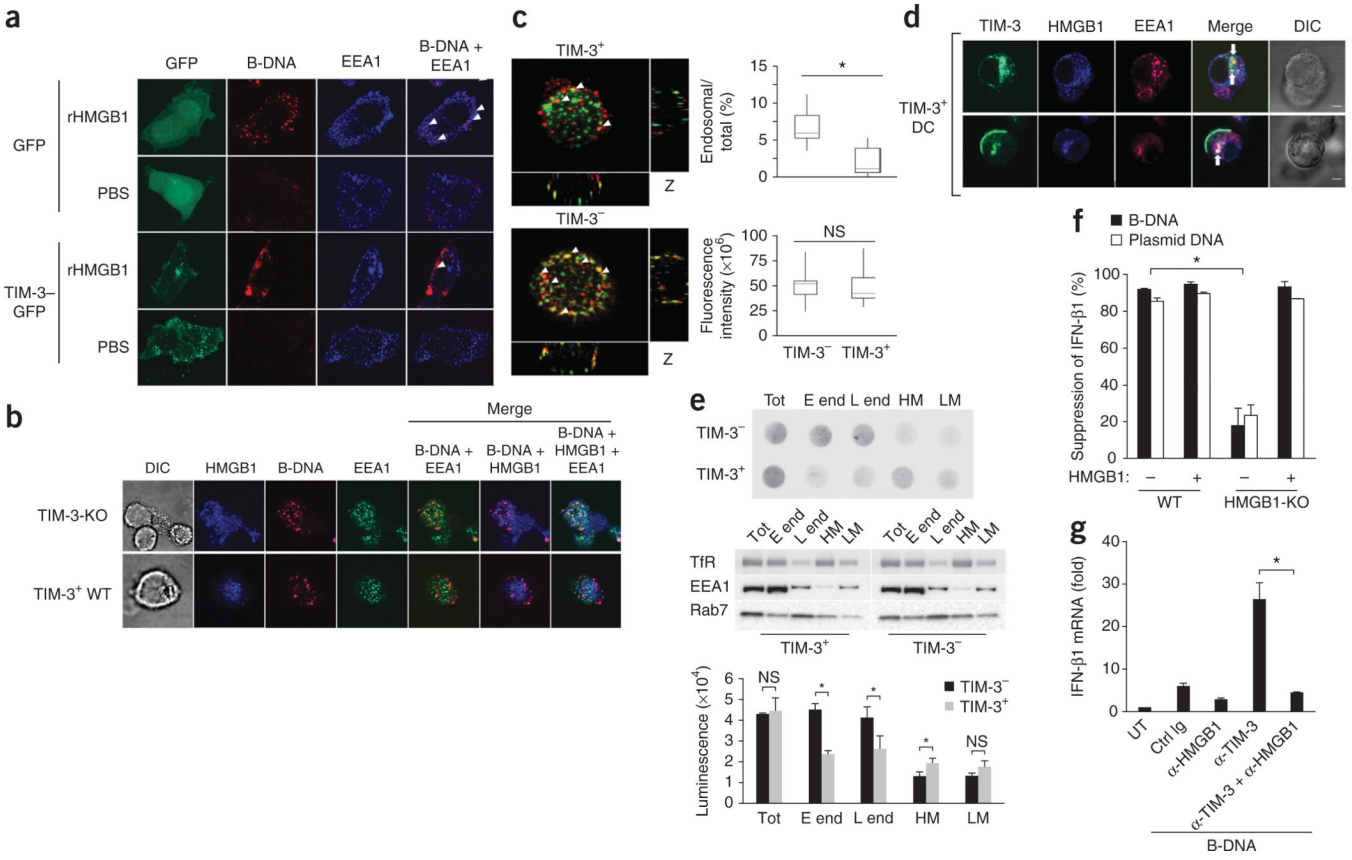

Figure 7.

TIM-3 inhibits the recruitment of nucleic acids into endosomes. (**a**) Microscopy of HMGB1-deficient MEFs transfected to express green fluorescent protein alone (GFP) or green fluorescent protein–tagged TIM-3 (TIM-3–GFP), then treated with recombinant HMGB1 (rHMGB1) or PBS, assessing the localization of B-DNA (red) in EEA1$^+$ endosomes (blue). Original magnification, ×1,000. (**b**) Confocal microscopy of TIM-3-deficient DCs and TIM-3$^+$ wild-type DCs 'loaded' with recombinant HMGB1 (blue), then stimulated with B-DNA, assessing the localization of B-DNA (red) in EEA1$^+$ endosomes (green). Original magnification, ×1,000. (**c**) Quantification of the fluorescence intensity of total cellular B-DNA (red (left); bottom right) and B-DNA in EEA1$^+$ endosomes (green (left)) relative to total cellular B-DNA (top right) in wild-type TIM-3$^+$ or TIM-3$^-$ BMDCs in images (left) acquired from the bottom to the top of the cells in **b**. Original magnification, ×1,200. (**d**) Confocal microscopy of the localization of TIM-3 (green) and HMGB1 (blue) in EEA1$^+$ endosomes (red) in TIM-3$^+$ DCs. Original magnification, ×1,000. (**e**) Dot-blot analysis of B-DNA (top) and immunoblot analysis of transferrin receptor (TfR), EEA1 and the late endosome marker Rab7 (middle) in total lysates (Tot), early endosomes (E end), late endosomes (L end) and heavy (HM) or light (LM) plasma membrane fractions isolated from homogenized BMDCs 2 h after treatment with B-DNA. Bottom, quantification of the dot-blot results above. (**f**) Suppression of IFN-β1 in wild-type or HMGB1-deficient (HMGB1-KO) MEFs transfected to express TIM-3, followed by stimulation with B-DNA or control plasmid DNA with (+) or without (–) recombinant HMGB1; results are presented relative to those of cells transfected with control vector. (**g**) RT-PCR analysis of IFN-β1 mRNA in TIM-3$^+$ BMDCs left untreated or pretreated with isotype-matched control immunoglobulin or anti-HMGB1 and/or mAb to TIM-3 (horizontal axis), followed by stimulation for 8 h with B-DNA; results are presented relative to *Actb* expression. *$P < 0.05$ (paired Student's *t*-

test). Data are representative of four experiments (**a**), three experiments (**b,e–g**) or five experiments (**d**) or are pooled from three separate experiments with 30 cells (**c**; error bars (**c,e–g**), s.e.m.).

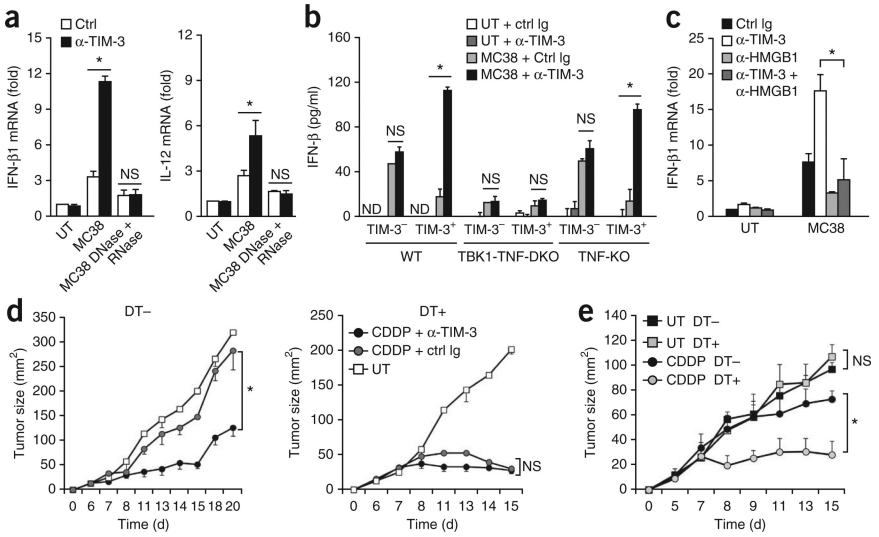

Figure 8.

TIM-3 impedes the antitumor effects of chemotherapy. (**a**) Quantification of IFN-β1 and IL-12 mRNA in TIM-3$^+$ BMDCs cultured alone (UT) or together with apoptotic CDDP-treated MC38 cells with (MC38 DNase + RNase) or without (MC38) pretreatment with DNase and RNase in the presence of control immunoglobulin or mAb to TIM-3; results are presented relative to *Actb* expression. (**b**) ELISA of IFN-β1 in TIM-3$^-$ and TIM-3$^+$ wild-type BMDCs (WT), BMDCs deficient in TBK1 and TNF (TBK1-TNF-DKO) or TNF-deficient BMDCs (TNF-KO) cultured alone or together withdying MC38 cells in the presence of control immunoglobulin or mAb to TIM-3. (**c**) RT-PCR quantification of IFN-β1 and IL-12 mRNA in wild-type TIM-3$^+$ DCs cultured alone or together with dying MC38 cells in the presence of control immunoglobulin or mAb to TIM-3 and/or anti-HMGB1 (key); results are presented relative to *Actb* expression. (**d**) Tumor growth in CD11c-DTR mice given no diphtheria toxin or treated with diphtheria toxin, then inoculated subcutaneously with MC38 cells along with systemic CDDP in the presence of mAb to TIM-3 or control immunoglobulin, or no treatment. (**e**) Tumor growth in chimeras reconstituted with a mixture (1:1) of bone marrow cells from CD11c-DTR and TIM-3-deficient mice, then given no treatment with diphtheria toxin or treated with diphtheria toxin 2 d before inoculation with MC38 cells, followed by no treatment or CDDP on days 8, 10 and 12 after inoculation. *$P < 0.05$ (paired Student's *t*-test). Data are representative of four experiments (**a**), five experiments (**b**) or three experiments (**c–e**; error bars, s.e.m.).